Agent based Simulations of Epidemics on a Large Scale
*Toward the Right Choice of Parameters**

Robert Elsässer[1], Adrian Ogierman[2] and Michael Meier[2]
[1]*Department of Computer Sciences, University of Salzburg, A-5020 Salzburg, Austria*
[2]*Institute for Computer Science, University of Paderborn, 33102 Paderborn, Germany*

Keywords: Epidemic Algorithms, Power Law Distribution, Disease Spreading, Public Health.

Abstract: In a world where epidemic outbreaks may take many lives, forecasting and analysis tools are of high importance - for an urban area such as New York City, a continent like Africa, as well as for the world itself. Such tools provide valuable insight on different levels and help to establish and improve embankment mechanisms. In this paper, we present an agent-based algorithmic framework to simulate the spread of epidemic diseases. Based on the population structure of Germany, we investigate the impact of the number of agents, representing the population, on the quality of the simulation. Real world data provided by the Robert Koch Institute (Arbeitsgemeinschaft Influenza, 2011; Robert Koch Institute, 2012) is used to evaluate our results. In a second step we empirically analyze the effects of certain non-pharmaceutical countermeasures as applied in the USA against the Influenza Pandemic in 1918-1919 (Markel et al., 2007). Our simulation and evaluation tool partially relies on the probabilistic movement model presented in (Elsässer and Ogierman, 2012). Based on our empirical tests, we conclude that the amount of agents in use can have a huge impact on the accuracy of the achieved simulation results. This reveals several challenges, which have to be taken into account in the design of forecasting and analysis tools for the spread of epidemics. On the other hand, we show that by utilizing the right parameters in our algorithmic framework - some of them being obtained from real world observations (Eubank et al., 2004) - one can efficiently approximate the course of a disease in real world.

1 INTRODUCTION

In order to improve our chances to control an epidemic outbreak, we need proper models which describe the spread of a disease. Institutes, governments, and scientists all over the world work intensively on forecasting systems to be well prepared if an unknown disease appears.

In recent years a huge amount of theoretical and experimental study has been conducted on this topic. While theoretical analysis provides important and sometimes even counter intuitive insights into the behavior of an epidemic (e.g. (Borgs et al., 2010; Elsässer and Ogierman, 2012)), in an experimental study one can take many different settings and parameters (Lee et al., 2008; Lee et al., 2010) into account. These usually cannot be considered simultaneously in a mathematical framework. A specific topology, for example, may have its own attributes that are completely different in other topological settings. Small islands connected only by ferries obviously offer other spreading opportunities than a huge metropolitan city. Furthermore, the characteristics of the spread of an epidemic also depend on the behavior of the infected individuals. That is, different people spread the disease (in its early stage) in different ways, which may or may not lead to an outbreak.

The goal of this paper is to present and empirically analyze a new dynamic model for the spread of epidemics. One of our objectives is to find the right parameters, which lead to realistic settings. Therefore, we investigate a general simulation environment, in which the different parameters can easily be adjusted to real world observations. A second objective is to evaluate similarities between countermeasure approaches in our model and the real world. We use empirical data for the comparison. Our tool is agent-based, i.e., the individuals (or groups of such) are modeled by agents interacting with each other. The environment approximates the geography of Germany, in which agents may travel between cities.

*Partially supported by the Austrian Science Fund (FWF) under contract P25214 and by DFG project SCHE 1592/2-1.

Elsässer R., Ogierman A. and Meier M..
Agent based Simulations of Epidemics on a Large Scale - Toward the Right Choice of Parameters.
DOI: 10.5220/0004429402630274
In *Proceedings of the 3rd International Conference on Simulation and Modeling Methodologies, Technologies and Applications* (SIMULTECH-2013), pages 263-274
ISBN: 978-989-8565-69-3

Within a city the agents interact according to the probabilistic model presented in (Elsässer and Ogierman, 2012) in a distributed manner. For a detailed description of the algorithmic framework see Section 2.

1.1 Related Work

There is a huge amount of work focusing on the analysis of epidemic diseases. In this subsection we provide an overview of the results which are closely related to the topic of this paper. In our description, we often rely on the style and wording of (Elsässer and Ogierman, 2012).

The structure of this subsection is as follows. At the beginning we present a simple model, which is often used to simulate an epidemic. Then, we describe some movement models, on which several studies w.r.t. the spread of epidemics are based. We conclude the section by providing an overview of certain empirical results in the field of disease spreading as well as of the main approaches one can identify.

There is plenty of work considering epidemiological processes in different scenarios and on various networks. The simplest model of mathematical disease spreading is the so called SIR model (see e.g. (Hethcote, 2000; Newman, 2003)). The population is divided into three categories: susceptible (S), i.e., all individuals which do not have the disease yet but can become infected, infective (I), i.e., the individuals which have the disease and can infect others, and recovered (R), i.e., all individuals which recovered and have permanent immunity (or have been removed from the system). Most papers model the spread of epidemics using a differential equation based on the assumption that any susceptible individual has uniform probability β to become infected from any infective individual. Furthermore, any infected player recovers at some stochastically constant rate γ.

This traditional (fully mixed) model can easily be generalized to a network. It has been observed that the corresponding process can be modeled by bond percolation on the underlying graph (Grassberger, 1983; Newman, 2002). Interestingly, for certain graphs with a power law degree distribution, there is no constant threshold for the epidemic outbreak as long as the power law exponent is less than 3 (Newman, 2003) (which is the case in most real world networks, e.g. (Faloutsos et al., 1999; Adamic and Huberman, 2000; Amaral et al., 2000; Ripeanu et al., 2002)). If the network is embedded into a low dimensional space, or has high transitivity, then there might exist a non-zero threshold for certain types of correlations between vertices (Newman, 2002). However, none of the papers above considered the dynamic movement of individuals, which seems to be the main source of the spread of diseases in urban areas (Eubank et al., 2004).

In (Eubank et al., 2004) the physical contact patterns are modeled by a dynamic bipartite graph, which results from movement of individuals between specific locations. The graph is partitioned into two parts. The first part contains the people who carry out their daily activities moving between different locations. The other part represents the various locations in a certain city. There is an edge between two nodes, if the corresponding individual visits a certain location at a given time. Obviously, the graph changes dynamically at every time step.

In (Eubank et al., 2004; Chowell et al., 2003) the authors analyzed the corresponding network for Portland, Oregon. According to their study, the degrees of the nodes describing different locations follow a power law distribution with exponent around 2.8[2]. For many epidemics, transmission occurs between individuals being simultaneously at the same place, and then people's movement is mainly responsible for the spread of the disease.

The authors of (Elsässer and Ogierman, 2012) considered a dynamic epidemic process in a certain (idealistic) urban environment incorporating the idea of attractiveness based distributed locations. The epidemic is spread among n agents, which move from one location to another. In each step, an agent is assigned to a location with probability proportional to its attractiveness. The attractiveness' of the locations follow a power law distribution (Eubank et al., 2004). If two agents meet at some location, then a possible infection may be transmitted from an infected agent to an uninfected one. The authors obtained two results. First, if the exponent of the power law distribution is between 2 and 3, then at least a small (but still polynomial) number of agents remains uninfected and the epidemic is stopped after a logarithmic number of rounds - even if each agent may spread the disease for $f(n)$ time steps (where $f(n) = o(\log n)$). Secondly, if the power law exponent is increased to some large constant, which is argued to be an implication of certain countermeasures against the spreading process, then the epidemic will only affect a polylogarithmic number of agents and the disease is stopped after $(\log\log n)^{O(1)}$ steps. In this case each agent is allowed to spread the disease for a number of time steps, which is bounded by some large constant. The results explain possible courses of a disease and point out why cost-efficient countermeasures may reduce

[2]In (Eubank et al., 2004) the degree represents the number of individuals visiting these places over a time period of 24 hours.

the number of total infections from a high percentage of the population to a negligible fraction.

In addition to the theoretical papers described above, plenty of simulation work has also been done. Two of the most popular directions are the so called agent-based and structured meta-population-based approach, respectively (cf. (Ajelli et al., 2010; Jaffry and Treur, 2008)). Both models have their advantages and weaknesses. The main idea of the meta-population approach is to model whole regions, e.g. georeferenced census areas around airport hubs (Balcan et al., 2009), and connect them by a mobility network. Then, within these regions the spread of epidemics is analyzed by using the well known mean field theory.

The agent-based approach models individuals with agents in order to simulate their behavior. In this context, the agents may be defined very precisely, including e.g. race, gender, educational level, etc. (Lee et al., 2008; Lee et al., 2010), and thus provide a huge amount of detailed data conditioned on the agents setting. Furthermore, these kinds of models are also able to integrate different locations like schools, theaters, and so on. Thus, an agent may or may not be infected depending on his own choices and the ones made by agents in his vicinity. The main issue of the agent-based approach is the huge amount of computational capacity needed to simulate huge cities, continents or even the world itself (Ajelli et al., 2010). This limitation can be attenuated by reducing the number of agents, which then entails a decreasing accuracy of the simulation. In the meta-population approach the simulation costs are lower, sacrificing accuracy and some kind of noncollectable data.

To combine the advantages of both systems, hybrid environments were implemented (e.g. (Bobashev et al., 2007)). The main idea of such systems is to use an agent-based approach at the beginning of the simulation up to some point where a suitable amount of agents is infected. Then, the system switches to a meta-population-based approach. Certainly, such a system combines the high accuracy of the agent-based simulations at the beginning of the procedure with the faster simulation speed of the meta-population-based approach at stages in which both systems may provide similar predictions. Here, the situation to switch between both approaches (in both directions) is defined by a threshold T describing a specific amount of infected agents. In (Bobashev et al., 2007), the authors compared average epidemic trajectories produced by both approaches and determined which threshold value (if any) results in equivalent average trajectories. For certain epidemics, especially unknown ones, this adjustment may be difficult or even not feasible at all.

These kind of simulations are also used to investigate the impact of (non-)pharmaceutical countermeasures on the behavior of an epidemic. Germann et al. (Germann et al., 2006) investigated the spread of a pandemic strain of the influenza virus through the U.S. population. They used publicly available 2000 U.S. Census data to identify seven so-called mixing groups, in which each individual may interact with any other member. Each class of mixing group is characterized by its own set of age-dependent probabilities for person-to-person transmission of the disease. They considered different combinations of socially targeted antiviral prophylaxis, dynamic mass vaccination, closure of schools and social distancing as countermeasures in use, and simulated them with different basic reproductive numbers R_0. It turned out that specific combinations of the countermeasures have a different influence on the spreading process. For example, with $R_0 = 1.6$ social distancing and travel restrictions did not really seem to help, while vaccination limited the number of new symptomatic cases per 10,000 persons from ~ 100 to ~ 1. With $R_0 = 2.1$, such a significant impact could only be achieved with the combination of vaccination, school closure, social distancing and travel restrictions.

1.2 Our Results

The results of this paper are two-fold. First, we show that by increasing the number of agents we are able to significantly improve the accuracy of our results in the scenarios we have tested. This is due to different phenomena, which are only visible if the amount of agents in use is large enough. For example, if the number of agents exceeds a certain value, then the epidemic manages to keep a specific (low) amount of infected individuals over a long time period. Furthermore, the number of agents has to be above some threshold to allow the epidemic to enter some specific areas/cities in the environment we used. Obviously, a certain amount of agents is also needed to avoid significant fluctuations in our results. However, we could not determine the right threshold for the specific instances, which certainly depends on the properties of the simulated environment and the population size.

The second main result of this paper is that by setting the parameters properly, one can approximate the effect of some non-pharmaceutical countermeasures, which are usually adopted if an epidemic outbreak occurs. This observation is supported by the empirical study of (Markel et al., 2007). Interestingly, the right choices of parameters in our experiments seem to be in line with previous observations in

real world (e.g. the right power law exponent seems to be in the range 2.6-2.9, cf. (Eubank et al., 2004)). To analyze the effect of the countermeasures mentioned above, we integrate the corresponding mechanisms on a smaller scale, and then verify their impact on a larger scale too.

2 THEORETICAL MODELS AND ALGORITHMIC FRAMEWORK

Our model is based on the distributed algorithmic framework introduced in (Elsässer and Ogierman, 2012). In that paper a (rough) asymptotic analysis of the spread of a disease in a large urban environment was considered, while in our paper we include its spread on a larger scale with several hundred cities, and provide a more precise (empirical) analysis on a smaller as well as on a larger scale. Hereby, the cities are chosen from a list in descending order of their population size. Since we do not consider cities inhabiting less than one agent on expectation, the number of agents is the limiting factor here. It is intuitively clear that large (and thus attractive) cities play a major role in a fast spread of an epidemic since a higher population density entails a potentially higher infection probability. Excluding such hotspots would of course slow down the infection spread. The problem is, this could only be achieved by quarantine the whole city itself. One cannot assume inhabitants living and working there would or could leave everything behind. Therefore we consider such strategies only on a smaller scale.

In our model, the agents may not only move between locations within a city but between cities as well. Furthermore, due to simplicity the agents are not categorized (i.e., they do not provide further properties like gender etc.). Note, we are not interested in the evaluation of such details. In the following, we briefly introduce the model.

Environment and Movement. Our model incorporates both intra- and inter-city movement. We model the inter-city movement using a complete graph $G = (V,E)$. In this graph, each $c \in V$ corresponds to a city of Germany. However, depending on the size, not every city is contained in V. The population is represented by $n = \sum_{c \in V} n_c$ agents, with n_c being the number of agents assigned to c proportional to its real world population. Furthermore, each city contains a number of so called *cells* described below. Agents may move independently from one cell to another or even travel to another city in each step. Each city $c \in V$ is assigned an attractiveness d_c proportional to its population size (w.r.t. the whole population). Note, afterwards d_c does not change anymore. Let $A_{i,s,t}$ be the event that agent i travels from city s to t. Let further p be the probability that an agent decides to travel at all, and let $dist(s,t)$ be the Euclidean distance between cities s and t. Then, the probability that event $A_{i,s,t}$ occurs is given by

$$Pr(A_{i,s,t}) = p \cdot \frac{d_t \cdot dist^{-1}(s,t)}{\sum_{(s,j) \in E} d_j \cdot dist^{-1}(s,j)}.$$

Thus, the probability for an agent entering a specific city is governed by the distance to said city, its population size as well as the current position of the considered agent.

Since our model incorporates intra-city movement as well, each $c \in V$ is a clique of cells on its own. These cliques are defined by $G_c = (V_c, E_c)$ with κn_c being the size of V_c (recall that n_c is the number of agents assigned to city c). Note, κ does not affect the amount of agents but the amount of cells only. The nodes $v \in V_c$ are the *cells* described above. Here, $\kappa > 0$ is a constant, which will be specified in the upcoming experiments. The cells represent locations within a city an agent can visit. Each cell may contain agents (individuals), depending on the cells so called *attractiveness*. The *attractiveness d* of a cell v is chosen randomly with probability proportional to $1/d^{\alpha}$, where $\alpha > 2$ is a constant depending on the simulation run. In each step, if an agent decides not to visit another city, then it moves to a randomly chosen cell according to the distribution of the attractiveness' among the cells. This also holds for the first cell an agent is accommodated in after entering a city.

Epidemic. We use three different states to model the distributed spreading process. These states partition the set of agents into three groups; $I(j)$ contains the infected agents in step j, $\mathcal{U}(j)$ contains the uninfected (susceptible) agents in step j, and $\mathcal{R}(j)$ contains the resistant agents in step j. Whenever it is clear from the context, we simply write I, $\mathcal{U}$, and $\mathcal{R}$, respectively. If at some step j an uninfected agent i visits a cell (within a city) which also contains agents of $I(j)$, then i becomes infected with probability $1-(1-\gamma)^{I'(j)}$, with $I'(j)$ being the number of infected individuals in the same cell. We refer to the concrete value of γ in the upcoming simulations.

Countermeasures. In our model, the countermeasures are governed by the parameters α and κ. That is, high values of these two parameters imply a high

level of countermeasures and vice-versa. With countermeasures applied, individuals avoid places with a large number of persons more often, waive needless tours, and are more careful when meeting other people. While α is mostly responsible for a decreasing number of visitors within a cell, and thus for the avoidance of crowded areas for example, κ governs the total space available for all individuals. That is, if κ increases, then more cells are available for the total number of individuals, and meetings within the same cell are less frequent. Thus, κ basically models how careful people interact with each other when they meet. As pointed out in (Markel et al., 2007), a single countermeasure alone is most likely not sufficient to stop an epidemic. Therefore, we assume a combination of countermeasures to be in place, which then would be able to sufficiently influence the parameters α and κ. Although the models described above already provide everything needed to simulate the use of countermeasures, one aspect is still missing. When do we activate/deactivate the countermeasures and what order of magnitude should they have? We use two different types of countermeasure-models for this purpose: a (multi-tier) *level based approach* considering the amount of infected agents in the current step, and a *ratio based approach* considering the amount of newly infected agents in the current step compared to the one in the step before. In the following, we use α_0 and κ_0 as initial values for α and κ, respectively.

In the level based model, we have one or more levels, and within each level a certain pair of parameters α and κ is used. Let LM_m stand for the level based model with m levels $L = \{l_1,...,l_m\} \cup l_0$. Further, let $T = \{l_0^d, l_0^u, l_1^d, l_1^u, ..., l_m^d, l_m^u\}$ be the set defining the transition points for all levels, i.e., l_i^d defines the transition point from level i to $i-1$ whereas l_i^u defines the transition point from level i to $i+1$. Note, $l_i^u = l_{i+1}^d$ does not necessarily hold. Additionally, $\alpha_0, \alpha_1, ..., \alpha_m$ and $\kappa_0, \kappa_1, ..., \kappa_m$ define the parameters α and κ, which are applied in the corresponding levels $l_0, \ldots, l_m$. For example, model LM_2 uses 2 levels. Let us assume that $l_0^d = 0, l_0^u = l_1^d = 10, l_1^u = l_2^d = 20, l_2^u = \infty$. That is, if at most 10 percent of the population of a city is infected in step i, α_0 and κ_0 are applied to simulate the spread of the disease. If the number of infected individuals is larger than 10 percent, then α_1 and κ_1 are used. Should the amount of infections go even above 20 percent, both parameters are raised to α_2 and κ_2, respectively. Similarly, both parameters are lowered to the previous values whenever the amount of infections falls below the corresponding transition values.

In contrast, the ratio based model *RM* uses a non static approach. Let the set of newly infected nodes of a city c in step i be denoted by $I_c^*(i)$. Furthermore, let α_i and κ_i denote the corresponding parameters used in step i. If $\frac{|I_c^*(i)|}{|I_c^*(i-1)|} \geq a$, for some constant a, then we set $\alpha_{i+1} = \alpha_i + z_1$ and $\kappa_{i+1} = \kappa_i + z_2$, where z_1, z_2 are some small constants which will be specified later. Consequently, if $\frac{|I_c^*(i)|}{|I_c^*(i-1)|} \leq 1/a$, then we set $\alpha_{i+1} = \max\{\alpha_0, \alpha_i - z_1\}$ and $\kappa_{i+1} = \max\{\kappa_0, \kappa_i - z_2\}$. The values applied in the various models are specified in Section 3.5.

3 EXPERIMENTAL ANALYSIS

As already stated in Section 1, the environment approximates the geography of Germany with up to 10 million agents. Note, the obtained results are almost identical for the same simulations utilizing 100 million agents. Depending on the number of agents, our simulations use several hundred cities as visitable areas spread all over the country. Each city is assumed to be reachable from any other city. However, an agent may travel at most 1000 km within a single time step. Each time step represents a whole day in the real world. Consequently, an agent moving from one city to another has to wait until its destination is reached before it can interact with other agents at its destination.

3.1 Setup and Implementation

The experiments, including the ones with 100 million agents, were mostly performed on a computation node of the Doppler cluster at the University of Salzburg. This node integrates a quad-socket AMD Opteron 6274 CPU (16 physical cores at 2.1 GHz each) with 512 GB RAM (32 x 16GB DIMMs). An Intel Xeon E5430 CPU (2,66 GHz, 4 physical cores) has been used as a secondary evaluation unit for experiments which were not so critical in terms of time.

Our simulator is implemented in Java and uses an agent-based core architecture, where each agent, depending on the number of overall agents in use, represents several inhabitants during the simulation. Furthermore, our system is completely event driven. Overall we are able to perform large scale experiments with more than 100 million agents in a reasonable time frame. Since such huge amounts of agents generate a significant impact in terms of performance, several parallelization approaches are implemented. For example, several worker threads are used, which are chosen accordingly to the number of available physical cores.Furthermore, to decrease the compu-

tational time for inter-city travels, we also take advantage of a parallelization approach concerning the agents themselves.

3.2 Simulations

In the upcoming sections we present and evaluate our results. Due to space limitations, only a selection of the results is presented here. In the following we focus on

1. the impact of the number of agents on the characteristics of the simulated epidemic compared to real world data, and
2. the impact of non-pharmaceutical countermeasures on the behavior of the epidemic (e.g. social distancing, school closures, and isolation (Markel et al., 2007)).

Furthermore, we also analyze our parameter settings. Although this is only a short part, our settings seem to coincide with the real world observations of (Eubank et al., 2004), and thus provide an additional valuable insight. Note that the figures presented in this section show values based on the real world population size and not on the number of agents. Thus, a direct comparability is given without the need to scale.

3.3 Relevance of the Chosen Parameters

Based on real world observations (e.g. (Eubank et al., 2004)), we chose $\alpha = 2.8$ and $\kappa = 1$ as a starting point for a series of simulations concerning α and κ, respectively. Each plot represents values averaged over 50 different simulation runs for each parameter constellation utilizing 10 million agents. The parameter notation is given in Table 1.

In Figure 1(a) and 1(b) we analyze the impact of α and κ on the behavior of the epidemic, and compare the results to the characteristics of a typical Influenza case reported by the RKI[3]. To increase the readability, we omit to add the RKI-plot as the 6th one. Instead we refer the reader to Fig. 2. Note, although the plots for $\alpha = 2.4$ and $\alpha = 2.6$ may seem more similar to the RKI-curve at first sight, the differences to the RKI-plot (cf. Table 2 for an example of similarity measures) are significant when scaled properly. Besides, of all five α-values $\alpha = 2.8$, which has also been obtained in (Eubank et al., 2004) in a different context, represents the best tradeoff between curve similarity and amount of infections. All remaining parameters were set to identical values as in Case 1 (cf. Section 3.4). For κ a similar phenomenon can be observed. With increasing κ (including fractional values), the characteristics of the curve (i.e., the amount of infected individuals at the peak vs. total number of infections and total duration of the outbreak) become less and less accurate. Even if we increase the value to 2, the obtained curve does not follow the characteristics of the real world observations reported by the RKI[3] anymore.

Table 1: The parameter notation used in the evaluation.

γ	With this probability an agent $v \in \mathcal{U}$ is being infected independently by each $w \in I$ occupying the same cell at the same time.
$D_I^{\uparrow}$	The amount of steps an agent $v \in I$ is infectious, thus being able to infect others.
$City_{init}$	Initial amount of cities the infection is being placed in.
$Agent_{init}$	Amount of initially infected agents which are placed in $City_{init}$ different cities.
α	The power law exponent used to compute the attractiveness of the cells within each city.
κ	A multiplicative factor to increase/decrease the amount of cells proportional to the initially assigned amount of agents. With $\kappa = 1$ the amount of agents is identical to the number of cells within each city.

In terms of the probability of infection γ we simply chose a reasonable value low enough to model an Influenza epidemic, but high enough to provoke an outbreak. This seemed reasonable due to the (at least to our knowledge) lack of concrete values deduced from real world observations.

3.4 Case 1 - Number of Agents

Before we present the results for this case, we first introduce the relevant sources for comparison. For Subcase a), we compare our results to real world data provided by the RKI (Robert Koch Institute, 2012) SurvStat system for the year 2007. The parameter values were taken from reference data provided by the RKI (Arbeitsgemeinschaft Influenza, 2011) where possible, or set to reasonable ones otherwise. In Subcase b) then, a disease for a fictional epidemic is presented.

3.4.1 RKI: Basis of Comparison

In this case, we compare our results to the real world data provided by the RKI[3]. For this purpose we use two different data sources: the official report of the

[3]The Robert Koch Institute (RKI) is the central federal institution in Germany responsible for disease control and prevention and is therefore the central federal reference institution for both, applied and response-orientated research. (Source: http://www.rki.de/EN/Home/homepage_node.html)

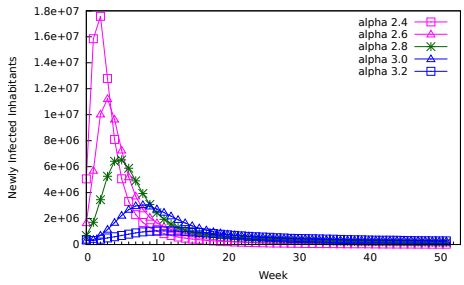

(a) $2.4 \leq \alpha \leq 3.2$

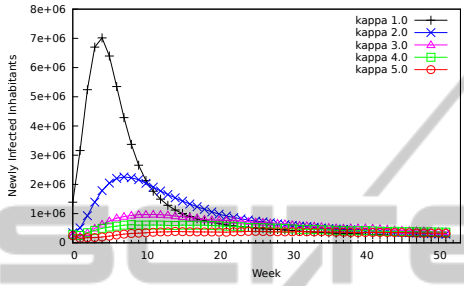

(b) $1 \leq \kappa \leq 5$

Figure 1: A composition of some simulation runs concerning varying α (1(a)) and κ (1(b)) only. All other parameters are identical to Case 1 (cf. Section 3.4). Each result represents the average of 50 different simulation runs with 10 million agents for the topology of Germany.

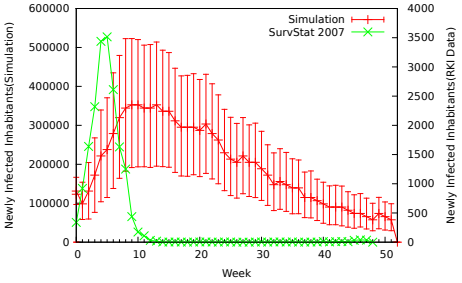

(a) 10.000 Agents

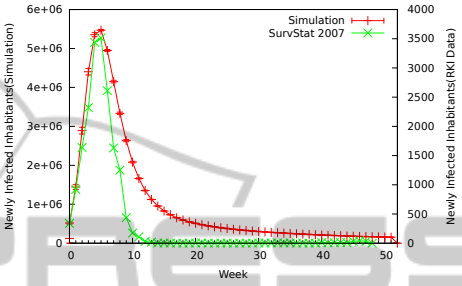

(b) 10.000.000 Agents

Figure 2: Simulation results for Case 1a) (red) in comparison to real world data (green) provided by the RKI for a varying amount of agents. Each result represents the average of 50 different simulation runs. The reliability of the averaged value is indicated by the corresponding confidence interval.

Influenza epidemiology of Germany for 2010/2011 (Arbeitsgemeinschaft Influenza, 2011) and an online database containing obligatory reports called SurvStat (Robert Koch Institute, 2012).

Relevance. The data for the SurvStat database and the report of 2010/2011 itself were obtained from more than 1% of all primary care doctors spread all over Germany. Note that not every infected person consults a doctor, which implies that the data of the SurvStat system contains only the serious courses of the disease. Nonetheless, these sources provide a valuable tool to obtain insight into the spread and persistence of the Influenza virus in Germany. Further, due to the data's significance, it is possible to estimate the number of infections within certain areas as well. Since the spread of infections in the real world is influenced by factors like seasonal fluctuations or the virus' aggressiveness, the number of total infections may significantly differ from year to year, cf. (Robert Koch Institute, 2012) for different years. However, the course of the curve usually does not change. Consequently, we do not focus on absolute values in our simulations, but on the *characteristics* of our results. These characteristics remain, up to some scaling factor, identical over the whole data set provided by the RKI.

3.4.2 Subcase a)

The Parameters in this case are as follows. We set $\gamma = 7\%$, $D_I^{\uparrow}$ to 5 days, the amount of initially infected cities $City_{init}$ to 1 (namely Berlin), and the amount of initially infected agents $Agent_{init}$ to 0.0015% of the overall agents used for these simulations. Furthermore, $\alpha = 2.8$ and $\kappa = 1$.

Each obtained plot represents the average of 50 different simulation runs. Figure 2 shows the results for the first subcase. Here, the green curve represents the real world data provided by the RKI for the year 2007 while the red curve represents our simulation results. Note that both curves vary significantly in terms of absolute numbers. However, this is not our focus here. Due to the level of abstraction in our model and since the RKI data only contains reported cases (see above), the absolute numbers do not coincide. Additionally, as stated above, the data provided by the RKI also differs significantly (in terms of absolute numbers but not the disease characteristics) from year to year (cf. (Robert Koch Institute, 2012)). Therefore, we focus on the course of the disease and the resulting characteristics of the plotted curves.

It is easy to see that the more agents are used, beginning from Figure 2(a) up to Figure 2(b), the more the curve characteristics converge. Moreover, the ac-

curacy of each simulation run increases as well (cf. the confidence intervals in Figure 2). With at least 500.000 agents in use, both curves become similar. Note that we shifted the outbreak position of the RKI data to the origin to create a comparable situation. Since the moment of an outbreak varies in reality as well (cf. (Robert Koch Institute, 2012)) and the beginning of the disease is not important for us, this relocation does not have any influence on the data or the evaluation itself.

To obtain a more formal evaluation, we define three measures, which are used to compare our results to the data provided by the RKI. These are: the time to peak (TTP), the epidemic duration (ED), and the area of the curve (AC). The time to peak describes the week with the maximum amount of newly infected agents of the corresponding curve. The area of the curve is simply the summation of the area between the origin and the endpoint EP (defined by the epidemic duration). Finally, the endpoint of the epidemic duration is the week in which only a minor amount of new infections occur, and no significant new infections are observed anymore. Minor infections are defined to start at a step i and last till the last step j of the simulation while for all steps $i \leq i' \leq j$ it holds that the amount of newly infected agents does not exceed 9% of the maximum value.

In Table 2 we consider the relative values of these measurements compared to the RKI data. That is, the numbers given in this table represent the ratio between the value obtained in our simulations and the value provided by the RKI. For example, a value of 4.00 for TTP in the case of 10.000 agents implies that the time to peak in our case divided by the time to peak in the real world data is 4.

Using the individual deviation measurements, we define a global deviation value by the formula $\frac{1}{3} \cdot \mathrm{TTP} + \frac{1}{3} \cdot \mathrm{AC} + \frac{1}{3} \cdot \mathrm{ED}$. For simplicity we consider each individual measurement uniformly weighted. The results, which confirm our previous observations, are given in Table 2 and Figure 3.

All obtained results and previous statements imply a fragile balance between the accuracy, the parameter setting, and the amount of agents in use.

3.4.3 Subcase b)

In Contrast to Subcase a), the Epidemic here is a Fictional One. We set $\gamma = 1.5\%$, $D_I^{\uparrow}$ to 5 days, the amount of initially infected cities $City_{init}$ to 1 (namely Berlin), and the amount of initially infected agents $Agent_{init}$ to 0.0015% of the overall agents used for these simulations. Furthermore, $\alpha = 2.8$ and $\kappa = 1$.

Table 2: Quantitative comparison and deviation measurements of the achieved results in Case 1a) with respect to the data provided by the RKI. The results refer to the following properties: time to peak (TTP), the epidemic dration (ED), and the area of the curve (AC). Here, the AC is starting at the origin and ending at the endpoint EP defined by the ED. All values are given as a relative deviation concerning the data provided by the RKI. The deviation value itself is computed utilizing $\frac{1}{3} \cdot \mathrm{TTP} + \frac{1}{3} \cdot \mathrm{AC} + \frac{1}{3} \cdot \mathrm{ED}$.

Agents	**Deviation** *TTP*	*ED / EP (week)*	*AC*	**Deviation Value**
10 K	2,33	3,53/53	5,58	3,81
25 K	2,00	3,53/53	4,71	3,41
50 K	1,83	3,47/52	3,70	3,00
100 K	1,33	2,87/43	3,10	2,43
250 K	1,17	2,27/34	2,59	2,01
500 K	1,17	1,87/28	2,29	1,77
1 M	1,17	1,67/25	2,16	1,66
2.5 M	1,00	1,53/23	2,00	1,51
5 M	1,00	1,47/22	1,92	1,46
10 M	1,00	1,40/21	1,88	1,43

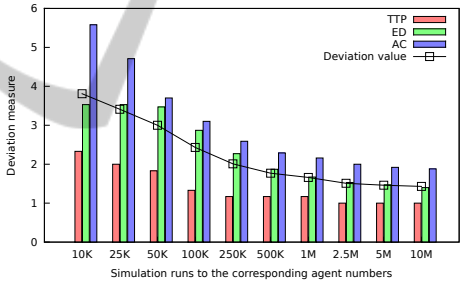

Figure 3: A visual representation of the data of Table 2.

In this subcase, we chose γ relatively low compared to the subcase above to emphasize the distortion. We show a significantly varying course of disease, which even exceeds the distortion of Subcase a). Using these parameters we were able to identify multiple curve characteristics, partially shown in Figure 4. The differences are significant. First, we observed the extinction of the disease almost instantly after the outbreak, followed by a completely unpredictable behavior including an increasing as well as a decreasing influence of the disease, up to a self-stabilizing infection spreading (cf. Fig. 4(a) and 4(b)). Since no other parameter was altered, only the different number of agents could have such a strong influence on the results.

Combined, both subcases indicate a significant influence of the amount of agents in use on the spreading process itself. One main goal in such simulations is to gain some speedup with a lower number

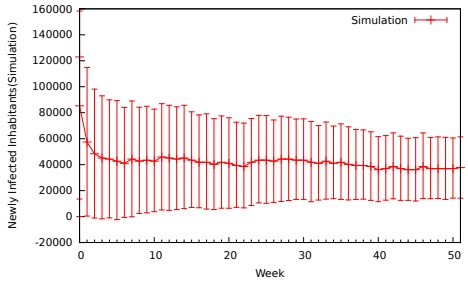

(a) 100.000 Agents

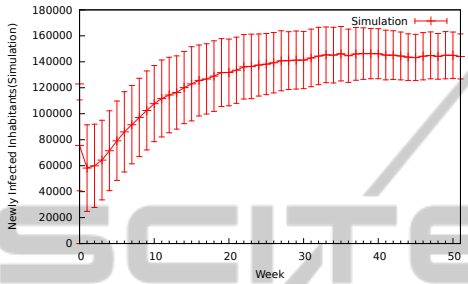

(b) 10.000.000 Agents

Figure 4: Simulation results for Case 1b) (red) for a varying amount of agents. Each result represents the average of 50 different simulation runs. The reliability of the averaged value is indicated by the corresponding confidence interval.

of agents while keeping the collectible data (for example the number of infections) almost identical in terms of accuracy. Now, this seems to be a very fragile premise which cannot necessarily be achieved. Note, we did not explicitly tune the settings for the different amount of agents since such possibilities may not be present or applicable for medical forecasting and disease estimation systems. Especially for unknown or largely unexamined diseases this may be very problematic. However, due to the dependency of the amount of cells in a city and the amount of agents in use, this is done, to some extent, implicitly by our model.

3.5 Case 2 - Non-pharmaceutical Countermeasures

Now we extend our analysis to incorporate non-pharmaceutical countermeasures such as school closures and social distancing. Here, we stick to a fictional epidemic simply because it simplifies the presentation, i.e., due to the increase of γ to 12%, a faster spread is achieved and the impact of the used countermeasures is amplified. Similar to Case 1, we set $D_I^{\uparrow}$ to 5 days, the amount of initially infected cities $City_{init}$ to 1 (namely Berlin), and the amount of initially infected agents $Agent_{init}$ to 0.00075% of the overall agents (to compensate the higher γ at the beginning). All relevant parameters concerning the countermeasure models can be found in Table 4 and 5.

We assume that such countermeasures basically affect the parameters α and κ, since the individuals will most likely avoid places with a large number of persons, waive needless tours, and be more careful when meeting other people. Although one of these modifications alone is most likely not sufficient (Markel et al., 2007), we can simply assume a combination of these strategies to be in place, which then would be able to sufficiently influence α and κ. For obvious reasons, we cannot compare our simulation results to current real world data, which consider different epidemics with varying (or no) countermeasures in use. Therefore, we use the work of Markel et al. (Markel et al., 2007) for this purpose. Especially Figure 5 is of particular interest. There, the direct correlation between establishing countermeasures and a decreasing amount of new infections (and vice versa) is well highlighted. We observed an identical effect in our simulations (cf. Figures 6, 7, 8 and Table 3). Note that different combinations of countermeasures used in (Markel et al., 2007) entail different kinds of impacts on the death rates. In contrast, we do not focus on specific combinations but on sufficient ones to actually achieve an immediate impact on the epidemic.

Table 3: Percentage of the overall infected inhabitants (Case 2). Column *NOCM* represents the percentage of overall infections without any countermeasures in use, whereas the other columns state the gain compared to the case without countermeasures for the corresponding level based and ratio based model, respectively.

Agents	**Infected Agents** *(in percent)*				
	NOCM	LM_1	LM_2	LM_3	*RM*
10 k	55,45	40,36	24,38	25,26	31,93
25 k	58.57	16,72	1,56	15,18	33,43
50 k	76,20	13,49	21,50	28,40	42,51
100 k	75,08	11,75	−0.29	16,50	27,88
250 k	81,37	11,13	18,95	16,38	40,30
500 k	85,77	18,05	16,15	20,04	39,26
1 M	86,12	1.84	14,53	12,16	37,41
2,5 M	88,22	12,47	14,66	13,42	35,47
5 M	87,39	11,33	8,50	8,90	29,81
10 M	88,06	8,0	9,30	9,15	32,08

As already described in Section 2, two different countermeasure approaches are of main interest for us: the level based (LM_1, LM_2 and LM_3), and the ratio based (*RM*), respectively. Both use different mechanisms and parameters to achieve the embankment of the epidemic. Recall that all transition points in the level based model are chosen w.r.t. the ratio between the amount of currently infected individuals and the population size of the city.

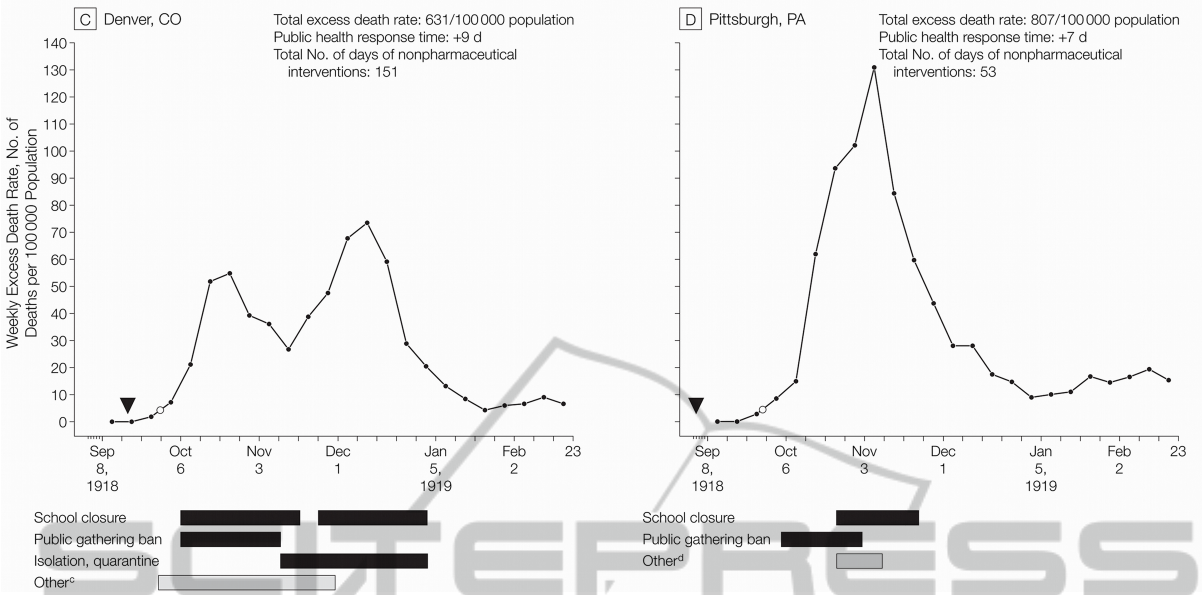

Figure 5: Weekly excess death rates from September 8, 1918, through February 22, 1919 (Markel et al., 2007, Figure 3).

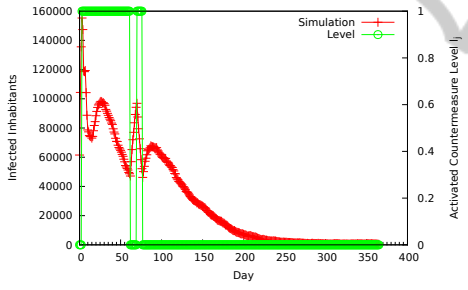

(a) Model LM_2, 10 million agents

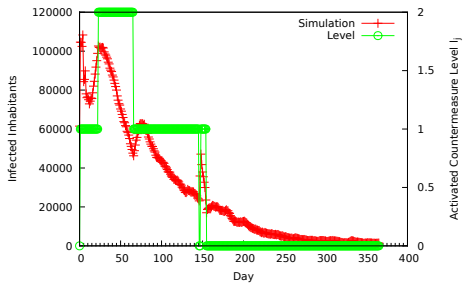

(b) Model LM_3, 10 million agents

Figure 6: Example results for BER for Case 2. The number of agents refers to the total amount in the simulation.

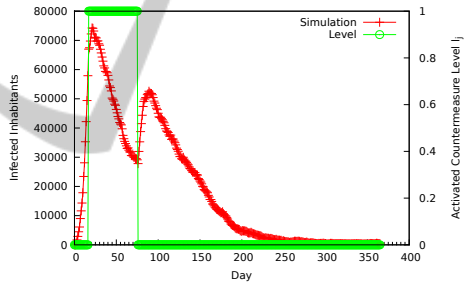

(a) Model LM_2, 10 million agents

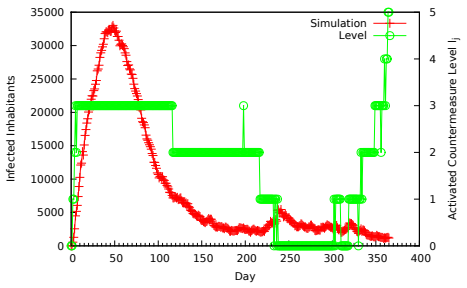

(b) Model RM, 10 million agents

Figure 7: Example results for HAM for Case 2. The number of agents refers to the total amount in the simulation.

Similar to Case 1, the results with at most 10 million agents in use are presented for each model. Although the level based approach is completely different compared to the ratio based approach, the achieved results are similar. However, the overall increase of α and κ by the ratio based approach may be noticeably higher, especially if a large number of agents is used (cf. for example Figure 8(b)). That is, while all LM-models use $\alpha \leq 3.3$, the RM-model goes above 4. This implies that the LM-models are more cost efficient, since both α and κ are kept lower and therefore less effort is needed to achieve and maintain said values.

Additionally, to be able to compare our results to

Table 4: Parameters for the level based countermeasure models relevant for Case 2.

Level	LM_1				LM_2				LM_3			
	l_i^u	l_i^d	α_i	κ_i	l_i^u	l_i^d	α_i	κ_i	l_i^u	l_i^d	α_i	κ_i
0	6%	0%	2.8	1.0	4%	0%	2.8	1.0	2%	0%	2.8	1.0
1	∞	4%	3.3	1.2	6%	2%	3.1	1.1	4%	1%	3.0	1.0
2	-	-	-	-	∞	4%	3.3	1.2	6%	2%	3.1	1.1
3	-	-	-	-	-	-	-	-	∞	4%	3.3	1.2

Table 5: Parameters for the ratio based countermeasure model relevant for Case 2.

RM Model				
a	z_1	z_2	α_0	κ_0
2	0.2	0.1	2.8	1.0

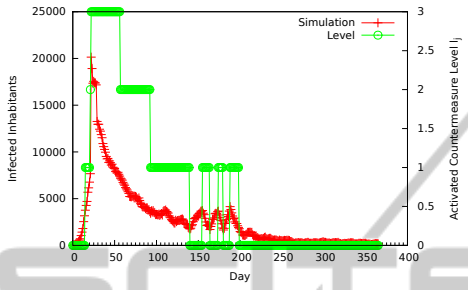

(a) Model LM_3, 10 million agents

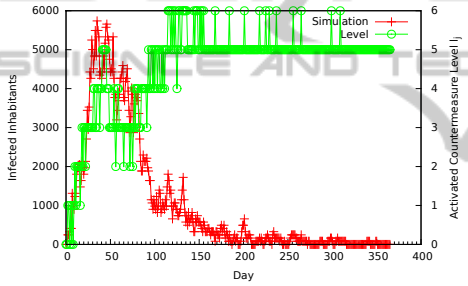

(b) Model RM, 1 million agents

Figure 8: Example results for PB for Case 2. The number of agents refers to the total amount in the simulation.

the findings in (Markel et al., 2007), we examine the following three cities in more detail: BER (population size: ≈ 3.5 million), HAM (population size : ≈ 1.8 million) and PB (population size: ≈ 146.000). Figures 6, 7 and 8 represent a composition of some interesting results for each city and model in use. Note that the green curve in these figures represents the countermeasure level for the *LM* models at the corresponding time, and indicates the number of times z_1, z_2 have increased α, κ in the *RM* model. Recall, in the *RM*-model level j implies $\alpha_i = \alpha_0 + \sum_{k=1}^{j} z_1$ and $\kappa_i = \kappa_0 + \sum_{k=1}^{j} z_2$ for a step i.

Our results confirm the impact, influenced by the effectiveness of the countermeasures, of different countermeasures observed in the real world (Markel et al., 2007). Compared to Figure 5, our simulations show a similar behavior (i.e., more than one peak during the epidemic). It is easy to see that the countermeasures presented in (Markel et al., 2007) directly influence the course of the epidemic. The same property can be observed in our results (cf. Figure 6(b), 7(a) or 8(a)). One can see that depending on the countermeasure level (indicated by the activated/used level), the number of infections increases or decreases. Note that although our figures show the number of infected individuals and not the death rate as shown in Figure 5, a comparison is still possible since this deviation can be normalized using a scaling factor.

Furthermore, we observe that small adjustments of the two parameters α and κ entail a significant impact on the number of overall infections (cf. Table 3). Among others, it was shown that if the power law exponent (and κ as well) is assumed to be some large constant, then even a very aggressive epidemic with $\gamma = 100\%$ will affect no more than a polylogarithmic number of the population. Our findings now back up these observations.

In conclusion, in this case we showed the impact of different countermeasures on the behavior of a population w.r.t. our model. Although some complexity of the real world is lacking, the similarities to real world observations are still present. Starting with settings for the environment, and therefore implicitly the individuals' behavior, based on real world observations (cf. Section 3.3) relatively low level countermeasures were sufficient to embank or at least significantly suppress an outbreak. Essentially the same properties were already observed in reality (cf. (Markel et al., 2007)). This underlines the importance of behavioral and environmental models based on power law distributions.

4 CONCLUSIONS

Agent based simulators offer various possibilities to perform very detailed experiments. However, the parameters used in these experiments highly influence the results one might obtain. As we have seen, even the number of agents has a significant impact on the quality of the results. This includes the reliability of different simulation runs with an identical parameter setting. By using the right parameter settings and a

proper number of agents, it is possible to approximate the course of a disease as observed in the real world. Furthermore, our experiments indicate that the algorithmic framework presented in this paper is able to describe, to some extent, the impact of certain non-pharmaceutical countermeasures on the behavior of an epidemic.

REFERENCES

Adamic, L. A. and Huberman, B. A. (2000). Power-law distribution of the world wide web. *Science*, 287(5461):2115.

Ajelli, M., Goncalves, B., Balcan, D., Colizza, V., Hu, H., Ramasco, J., Merler, S., and Vespignani, A. (2010). Comparing large-scale computational approaches to epidemic modeling: Agent-based versus structured metapopulation models. *BMC Infectious Diseases*, 10(190).

Amaral, L. A., Scala, A., Barthelemy, M., and Stanley, H. E. (2000). Classes of small-world networks. *PNAS*, 97(21):11149–11152.

Arbeitsgemeinschaft Influenza (2011). Bericht zur Epidemiologie der Influenza in Deutschland Saison 2010/11.

Balcan, D., Hu, H., Goncalves, B., Bajardi, P., Poletto, C., Ramasco, J. J., Paolotti, D., Perra, N., Tizzoni, M., den Broeck, W. V., Colizza, V., and Vespignani, A. (2009). Seasonal transmission potential and activity peaks of the new influenza A(H1N1): a Monte Carlo likelihood analysis based on human mobility. *BMC Medicine*, 7:45.

Bobashev, G. V., Goedecke, D. M., Yu, F., and Epstein, J. M. (2007). A hybrid epidemic model: combining the advantages of agent-based and equation-based approaches. In *Proc. WSC '07*, pages 1532–1537.

Borgs, C., Chayes, J., Ganesh, A., and Saberi, A. (2010). How to distribute antidote to control epidemics. *Random Struct. Algorithms*, 37:204–222.

Chowell, G., Hyman, J. M., Eubank, S., and Castillo-Chavez, C. (2003). Scaling laws for the movement of people between locations in a large city. *Physical Review E*, 68(6):661021–661027.

Elsässer, R. and Ogierman, A. (2012). The impact of the power law exponent on the behavior of a dynamic epidemic type process. In *Proc. SPAA'12*.

Eubank, S., Guclu, H., Kumar, V., Marathe, M., Srinivasan, A., Toroczkai, Z., and Wang, N. (2004). Modelling disease outbreaks in realistic urban social networks. *Nature*, 429(6988):180–184.

Faloutsos, M., Faloutsos, P., and Faloutsos, C. (1999). On power-law relationships of the internet topology. In *SIGCOMM '99*, pages 251–262.

Germann, T. C., Kadau, K., Longini, I. M., and Macken, C. A. (2006). Mitigation strategies for pandemic influenza in the United States. *PNAS*, 103(15).

Grassberger, P. (1983). On the critical behavior of the general epidemic process and dynamical percolation. *Mathematical Biosciences*, 63(2):157 – 172.

Hethcote, H. W. (2000). The mathematics of infectious diseases. *SIAM Review*, 42(4):599–653.

Jaffry, S. W. and Treur, J. (2008). Agent-Based and Population-Based Simulation: A Comparative Case Study for Epidemics. In Louca, L. S., Chrysanthou, Y., Oplatkova, Z., and Al-Begain, K., editors, *ECMS'08*, pages 123–130.

Lee, B. Y., Bedford, V. L., Roberts, M. S., and Carley, K. M. (2008). Virtual epidemic in a virtual city: simulating the spread of influenza in a us metropolitan area. *Translational Research*, 151(6):275 – 287.

Lee, B. Y., Brown, S. T., Cooley, P. C., Zimmerman, R. K., Wheaton, W. D., Zimmer, S. M., Grefenstette, J. J., Assi, T.-M., Furphy, T. J., Wagener, D. K., and Burke, D. S. (2010). A computer simulation of employee vaccination to mitigate an influenza epidemic. *American Journal of Preventive Medicine*, 38(3):247 – 257.

Markel, H., Lipman, H. B., Navarro, J. A., Sloan, A., Michalsen, J. R., Stern, A. M., and Cetron, M. S. (2007). Nonpharmaceutical Interventions Implemented by US Cities During the 1918-1919 Influenza Pandemic. *JAMA*, 298(6):644–654.

Newman, M. E. J. (2002). Spread of epidemic disease on networks. *Phys. Rev. E*, 66(1):016128.

Newman, M. E. J. (2003). The structure and function of complex networks. *SIAM Review*, 45(2):167–256.

Ripeanu, M., Foster, I., and Iamnitchi, A. (2002). Mapping the gnutella network: Properties of large-scale peer-to-peer systems and implications for system. *IEEE Internet Computing Journal*, 6(1):50–57.

Robert Koch Institute (2012). SurvStat@RKI. A web-based solution to query surveillance data in Germany.